# Investigating the Impact of Internal and External Convection on Thermal Explosion in a Spherical Vessel

A.N. Campbell, Lecturer, Department of Chemical and Process Engineering, Faculty of Engineering and Physical Sciences, University of Surrey, Guildford GU2 7XH

When any exothermic reaction proceeds in an unstirred vessel, natural convection may develop. The presence of this flow may alter the balance between heat generation and heat removal in the vessel, which ultimately governs whether the system will explode. Classical theories of thermal explosion have largely neglected the potentially important role that buoyant convection can play. More recently, numerical investigations of the effects of natural convection on thermal explosion have considered reactors where the temperature of the wall of the vessel is held constant. Thus, there is a physically unrealistic, infinitely fast heat transfer between the wall and the surrounding environment. In reality, there will be heat transfer resistances associated with conduction through the wall of the vessel and due to convective transfer from the surface arising from the local environmental conditions. These additional modes of heat transfer have the potential to fundamentally alter the rate of heat transfer from the hot zone in the vessel, to the cooler environment. This work presents a numerical study of thermal explosion in a spherical reactor under the influence of natural convection and external heat transfer, which neglects the effects of consumption of reactant. Simulations were performed to examine the changing behaviour of the system as the intensity of convection, as characterised by the Rayleigh number, and the importance of external heat transfer, as characterised by the Biot number, were varied. It was shown that the temporal development of the maximum temperature in the vessel was qualitatively similar as the Rayleigh and Biot numbers were varied. It has been shown that the maximum dimensionless temperature achieved in a non-explosive reaction on the explosion boundary increases from 1 in the well mixed limit to its constant wall temperature value asymptotically. For Bi < ~ 10, the maximum temperature varies little with Rayleigh number, but interestingly is lower for higher values of Ra. This is in contrast to what is observed at higher Bi where more intense natural convection means that higher temperatures can be sustained in non-explosive cases. Importantly, this variation in maximum temperature achieved in stable systems means that explosion criteria based on the maximum temperature achieved in the reactor may be inappropriate for systems with significant external heat transfer. Additionally, regions of parameter space where explosions occurred were identified. It was shown that reducing the Biot number increases the likelihood of explosion and reduces the stabilising effect of natural convection. The effects of varying important process parameters, such as the size of the vessel and the initial temperature and pressure of the gas on the tendency to explode are also shown. Finally, the results of the simulations were shown to compare favourably with analytical predictions in the classical limits of Semenov and Frank-Kamenetskii.

## Introduction

When any exothermic reaction occurs in a closed vessel then there is a risk of thermal explosion. Such explosions occur when the rate of heat production by the reaction exceeds the rate of heat removal through the vessel's walls. The pioneering works on thermal explosion by Semenov (1928) and Frank-Kamenetskii (1969) considered two extreme cases. Semenov investigated cases where the mixing within the vessel was so efficient that its contents could be considered to be spatially uniform. In contrast, Frank-Kamenetskii considered a case without mixing. In such a scenario, spatial temperature gradients develop. Frank-Kamenetskii realised that these gradients would significantly impact the heat removal from the system, and hence the tendency to explode. In particular, he considered cases where heat transfer occurred by conduction only.

If the temperature gradients become sufficiently large, the resulting buoyancy forces will cause the gas to move. This natural convection can have a significant influence on the progress of the reaction. The nature of the induced flow is determined by the Rayleigh number, $Ra = (\beta\, g\, L^3\, \Delta T) / (\kappa\, \nu)$. Frank-Kamenetskii (1969) suggested that in a gaseous system, natural convection becomes significant when $Ra > 10^4$; however, further studies (Tyler, 1966) have shown that natural convection becomes important when $Ra$ exceeds ~ 500.

The initial experimental evidence for a greater influence of natural convection than was allowed for by Frank-Kamenetskii in his model inspired a number of experimental and numerical investigations of exothermic reactions with natural convection. The experimental work of Merzhanov and Shtessel (1971) on liquid systems in a horizontal cylinder showed that natural convection is significant at Rayleigh numbers well below $10^4$. Jones (1973) noted that inside a horizontal cylinder or a sphere, there is always some convection, because of the existence of temperature gradients perpendicular to the gravity vector; the 'onset' of convection is in fact merely the point where the effects of this flow become observable. In a seminal work on the interaction of thermal explosion and natural convection, Merzhanov and Shtessel (1973) presented a detailed numerical and experimental analysis of explosion in a liquid system. They showed that natural convection suppresses explosion, and that when explosion does occur, the ignition delay is longer in the presence of natural convection.

In all of these numerical studies, the effect of $Ra$ on thermal explosion was quantified by calculating a new critical value of the Frank-Kamenetskii number, $\delta$. More recently, a new approach was proposed by Liu *et al.* (2008),who presented an analysis in which the explosive limits were described in terms of a series of ratios of characteristic timescales for the important physical processes that are at work, namely natural convection, diffusion (of both heat and mass) and heating due to the chemical reaction. This approach is very attractive, as it describes the transition to explosion in terms of simple groups, which have clear physical meaning. Significantly, Liu *et al.* (2010) also revisited the issue of defining when an explosion can be deemed to have occurred in a system with significant depletion of reactant. This transition to explosion is obvious in systems with minimal reactant consumption, where in an explosive case the temperature will increase without bound; however, when the reactant is depleted, this will significantly reduce the production of heat by the reaction. Consequently, a plot of the temporal development of the maximum temperature in the vessel will display a clear maximum.

Liu *et al.* (2010) proposed a simple criterion to determine whether an explosion has occurred based solely on the maximum dimensionless temperature achieved. When this exceeds 5, an explosion is said to have occurred.

Many other numerical studies have considered the effect of natural convection on explosion in so-called class A geometries (*i.e.* parallel plates, infinite cylinders and spheres). These studies, however, all consider cases in which the fixed boundaries of the reactor are held at a constant temperature. This constant temperature at the wall implies there is an infinite heat transfer coefficient between the reactor and its surroundings. In reality, this is unlikely to be the case. There will, of course, be a heat transfer resistance associated with conduction through the solid wall of the reactor, and a finite resistance between the wall and the environment. It is obvious that these additional heat transfer mechanisms may significantly alter the rate of heat removal from the reactor, and hence the tendency of the fluid to explode. Despite this important fact, very few studies have included the effect of external heat transfer in their analyses. Frank-Kamenetskii (1969) did derive an approximate expression for the dependence of $\delta$ in a purely diffusive system on external heat transfer, *via* what he called a Nusselt number, but what is in reality a Biot number. He found that the inclusion of a finite rate of external heat transfer made an explosion more likely. Boddington *et al.* (1984) performed an elegant asymptotic analysis of a purely diffusive system in which consumption of reactant is important. They showed that external heat transfer, again characterised by a Biot number, had a more significant effect in a spherical system, when compared with the other class A geometries.

This work aims to perform an initial investigation into the transition from a slow reaction to explosion in a spherical reactor in which natural convection is significant, but in which depletion of the reactant can be ignored. The governing equations are presented in section 2. The results of numerical simulations are discussed in section 4. In addition, the results are compared with the analytical results of Semenov and Frank-Kamenetskii.

## Theoretical Background

### Dimensional Equations

The reaction occurring in a spherical reactor is considered to be an $n^{\text{th}}$ order exothermic, thermal decomposition reaction, in which the concentration of the reactant is assumed to remain constant at its initial value, $c_0$. The governing equations express the conservation of the reactant, energy, momentum and mass. The Boussinesq approximation, in which density changes are ignored in all terms except the body forces (which drive natural convection) in the Navier-Stokes equations, is applied to considerably simplify the equations. This approach has been used extensively in the study of thermal explosion.

The conservation of energy within the reactor is described by:

$$\frac{\partial T}{\partial t} + \underline{u}.\nabla T = \kappa \nabla^2 T + \frac{qk(T)}{\rho_0 C_P} c_0^n , \tag{1}$$

where $C_P$ is the mixture's specific heat at constant pressure, $T$ is its temperature, $\kappa$ is the thermal diffusivity, $\rho_0$ is the density at the initial temperature $T_0$ and $q$ is the exothermicity of the reaction. The rate constant $k$ is assumed to have Arrhenius temperature dependence, *i.e.* it has the form $k = Z \exp(-E/RT)$, where $Z$ is the pre-exponential factor and $E$ is the activation energy. The familiar Navier-Stokes equations:

$$\frac{\partial \underline{u}}{\partial t} + \underline{u}.\nabla \underline{u} = -\frac{1}{\rho_0}\nabla(P - P_0) + \nu \nabla^2 \underline{u} + \frac{\rho - \rho_0}{\rho_0}\underline{g} , \tag{2}$$

describe conservation of momentum, where $P$ is the pressure in the reactor and $\nu$ is the kinematic viscosity. Per the Boussinesq approximation, the density only varies in the buoyancy term of Eq. (2), in which $\rho = \rho_0[1 - \beta(T - T_0)]$, where $\beta$ is the coefficient of thermal expansion.

The final equation required is the continuity equation. Adoption of the Boussinesq approximation allows the continuity equation to be written in its incompressible form, *i.e.*

$$\nabla.\underline{u} = 0 . \tag{3}$$

The gas is assumed to be initially motionless and at a uniform temperature $T_0$; this is the temperature of the surrounding environment, which remains fixed throughout the course of the reaction. The external resistance to heat transfer is modelled *via* a heat transfer coefficient, $h$. It is assumed that the no-slip condition applies at the wall and that there is no flux of any species at the wall. The effects of any heterogeneous reactions at the wall have hence been ignored. The initial and boundary conditions can thus be stated:

$$t = 0: \quad T = T_0;\ \underline{u} = 0 \quad \forall \underline{x}$$

$$\text{At the wall:} \quad \underline{u} = 0;\ \ \underline{n}.(-k_T \nabla T) = h(T - T_0), \tag{4}$$

where $\underline{n}$ is a unit vector perpendicular to the wall of the vessel and $k_T$ is the thermal conductivity of the gas.

### Dimensionless Equations

Following the method proposed by Liu *et al.* (2008) the governing equations (1) – (4) can be made dimensionless by the introduction of the following dimensionless variables:

$$c' = \frac{c}{c_0};\ T' = \frac{T - T_0}{\Delta T};\ \underline{u}' = \frac{\underline{u}}{U};\ P' = \frac{P - P_0}{\rho_0 U^2};\ \underline{x}' = \frac{\underline{x}}{L} \text{ and } t' = \frac{Ut}{L}, \tag{5}$$

where $\Delta T = RT_0^2/E$ is a characteristic scale for the rise in temperature due to the reaction, $U = (\beta g L \Delta T)^{1/2}$ is a characteristic velocity when natural convection dominates transport and $L$ is the characteristic length scale for the reactor, taken to be the radius in the present work. Additionally, the following characteristic timescales can be defined:

$$\tau_D = \frac{L^2}{\kappa};\ \tau_C = \frac{L}{U} \text{ and } \tau_H = \frac{\rho_0 C_P R T_0^2}{k_0 c_0^n q E}, \tag{6}$$

for diffusion, natural convection and heating due to the reaction, respectively. Here, $k_0$ is the rate constant evaluated at the initial temperature $T_0$. Equations (5) and (6) allow the governing equations (1) – (4) to be written as dimensionless form as:

$$\frac{\partial T'}{\partial t'} + \underline{u}'.\nabla' T' = \frac{\tau_C}{\tau_D}\nabla'^2 T' + \frac{\tau_C}{\tau_H}\exp\left(\frac{T'}{1+\eta T'}\right), \tag{7}$$

$$\frac{\partial \underline{u}'}{\partial t'} + \underline{u}'.\nabla'\underline{u}' = -\nabla' P' + Pr\,\frac{\tau_C}{\tau_D}\nabla'^2\underline{u}' - \frac{g}{g}T', \tag{8}$$

$$\nabla'.\underline{u}' = 0, \tag{9}$$

$$t' = 0:\quad T' = 0;\ \underline{u}' = 0 \quad \forall \underline{x}'$$

$$\text{At the wall}:\ \underline{u}' = 0;\quad -\underline{n}.\nabla' T' = Bi\,T', \tag{10}$$

where $Le = \kappa / D_C$ is the Lewis number, $T'_{ad} = qc_0E/(\rho_0 C_P R T_0^2)$, $\eta = RT_0/E$, $Pr = \nu/\kappa$ is the Prandtl number and $Bi = h L / k_T$ is the Biot number. The limiting cases of constant wall temperature and perfect mixing are represented by $Bi = \infty$ and $Bi = 0$, respectively. The governing dimensionless equations (7) – (9) are the same as those presented previsouly (Liu *et al.*, 2008), whilst the boundary conditions in equation (10) differ.

The behaviour of this system can therefore be characterised by the following five dimensionless groups:

$$\frac{\tau_H}{\tau_D}, \frac{\tau_H}{\tau_C}, \eta, Pr, Bi \tag{11}$$

and for a given chemical system, where $\eta$ and $Pr$ are fixed, then the behaviour of the system is governed by the ratios $\tau_H/\tau_D$ and $\tau_H/\tau_C$, as well as $Bi$. For a system with a constant wall temperature, the behaviour is only a function of the ratios of timescales as $Bi$ would be infinite. Thus the behaviour of the system can be characterised by a three dimensional regime diagram.

## Numerical Method

The governing equations (1) – (4) were solved using COMSOL Multiphysics® 4.3a (COMSOL, 2012), which utilises the finite element method. The solution was assumed to be axisymmetric about the vertical axis of the spherical vessel. Accordingly, the equations were solved on a semi-circular, 2-dimensional mesh consisting of approximately 3000 linear triangular elements. For the numerical simulations the thermal decomposition of azomethane was considered. The order of this reaction has been found experimentally as $n$ = 1.4. The physico-chemical properties employed were: $C_p$ = 2250 J kg$^{-1}$ K$^{-1}$, $Z = 1.24 \times 10^{14}$ mol$^{-0.4}$ m$^{1.2}$ s$^{-1}$, $E / R$ = 23280 K (so $E$ = 193.6 kJ mol$^{-1}$). The exothermicity of the reaction was assumed to be $q$ = 124 kJ mol$^{-1}$. In accordance with previous studies, the radius of the reactor was taken to be $L$ = 0.064 m, corresponding to a reactor with a volume of 1100 dm$^3$. The temperature of the environment was taken as $T_0$ = 636.2 K, which matches the wall temperature used in previous studies. The concentration of azomethane in the reactor was assumed to remain constant, as discussed above, with $c_0$ = 0.37 mol m$^{-3}$. The ratios $\tau_H/\tau_D$ and $\tau_H/\tau_C$ were varied by changing the value of $\kappa$ and $g$, respectively. The external heat transfer coefficient $h$ was then varied to give the desired $Bi$. Simulations were performed for $Ra < 10^6$, *i.e.* cases where the natural convection was laminar. The system was further simplified by assuming that $Pr$ = 1, *i.e.* the diffusivities of heat and momentum were assumed to be equal. This is approximately true for gasses but not for liquids.

## Results and Discussion

### Temporal and Spatial Development of the Temperature and Speed

The inclusion of an external heat transfer resistance alters the heat removal from the system. Additionally, the temperature of the wall is no longer constant throughout the duration of the reaction. Both of these factors may alter the way the reaction proceeds, and hence the spatial structures within the reactor. To investigate this difference, simulations were run to examine the difference between stable and explosive reactions at three different values of *Bi*. The values considered are *Bi* = 10 (where external heat transfer is significant, but internal resistances still dominate overall), *Bi* = 1 (where internal and external thermal resistances are similar in magnitude) and *Bi* = 0.1 (where external heat transfer is the dominant mechanism). Additionally, three intensities of natural convection, as characterised by *Ra* were considered: $Ra = 10^3$, where natural convection is becoming important, $Ra = 10^4$, where laminar convection is dominant and $Ra = 10^5$, where the system is approaching the transition to turbulence. Plotted in Fig. 1 are the temporal developments of the maximum dimensionless temperatures in the reactor for four cases at the extremes of the range of *Bi* and *Ra* considered.

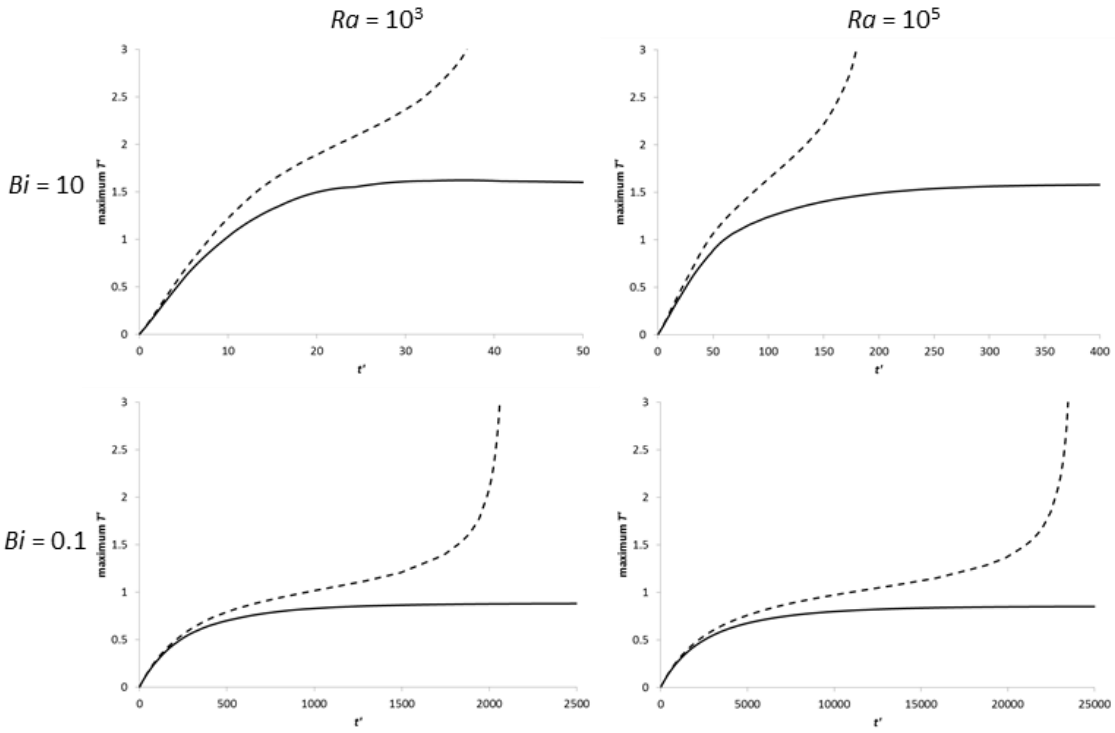


Figure 1. The temporal evolution of the maximum dimensionless temperature in the reactor for *Bi* = 10 and 0.1, when *Ra* = $10^3$ and $10^5$. These cases fall either side, but close to, the explosion boundary. The stable reactions are plotted as solid lines, whilst the explosive cases are dashed lines. The plots are ordered such that *Bi* is constant along a row and *Ra* is constant along a column.

For *Bi* = 10, it is clear that the temporal development of the stable cases is remarkably similar. In each case, the temperature rises at a relatively constant rate initially, before the rate of increase slows as the natural convection develops and enhances heat removal. When convection becomes fully established, the maximum temperature reaches its steady value. Interestingly, in both cases the maximum value at steady state is $T' \sim 1.5$. The explosive cases show a similar rise in temperature to the non-explosive cases initially. Unsurprisingly, after this initial period, the maximum temperature in the vessel is higher than is the case for the stable reactions. In all three cases there is clearly a decrease in the slope of the temperature *versus* time curve (*i.e.* $\partial^2 T'/\partial t'^2 < 0$) before an upward inflection in the curve, after which the temperature increases without bound. Such a shape of curve is, of course, characteristic of an explosive system in which reactant consumption is ignored. If consumption of reactant was important, then the increase in temperature would remain bounded, due to the limited heat production by the reaction of a finite mass. In each case, the inflection in temperature can be seen to occur when $T'$ is in the range 1.5 – 2. It has been noted previously (Liu *et al.*, 2008), that this upward inflection in temperature, which is often used to define whether or not an explosion has occurred, can be seen in non-explosive cases when natural convection is important. In particular, it is characteristic of cases where significant reaction occurs before natural convection has been established, and once the flow is significant, the heat removal at the wall increases and thus stabilises the reaction. It is also interesting to note that the dimensionless time to explosion increases with increasing *Ra*. The times for onset of convection and explosion have not been considered further here.

Similar trends are evident when comparing the stable and explosive cases for reduced values of *Bi*. When *Bi* = 0.1, *i.e.* when the heat transfer is largely controlled by the external resistance, the temperature at which the upward inflection is seen is lower than in those cases with higher *Bi* and the maximum temperature of the stable systems is lower $T' \sim 1$. Therefore,

comparison of all four explosive cases and all four stable cases reveals that the evolution of the maximum temperature in the vessel is qualitatively similar across the range of *Bi* and *Ra* considered. The most obvious quantitative difference is that the temperatures seen, both at the point where the explosive reaction accelerates to infinity and in the maximum temperature of the stable system, are smaller as *Bi* is increased, but remarkably similar as *Ra* is varied at fixed *Bi*.

It is clear from Fig. 1 that temporal development of the maximum temperature in the vessel is affected very little by either *Bi* or *Ra*, with the primary quantitative difference being in the magnitude of the temperatures observed. It is, however, to be expected that the spatial development of the temperature, and hence velocity fields will be more significantly altered by the existence of external heat transfer. Plotted in Fig. 2 are the spatial variations of the temperature and speed of the flow as explosive reactions proceed. Specifically, explosive cases for *Bi* = 10, 1 and 0.1 with *Ra* = $10^3$ and $10^5$ are considered.

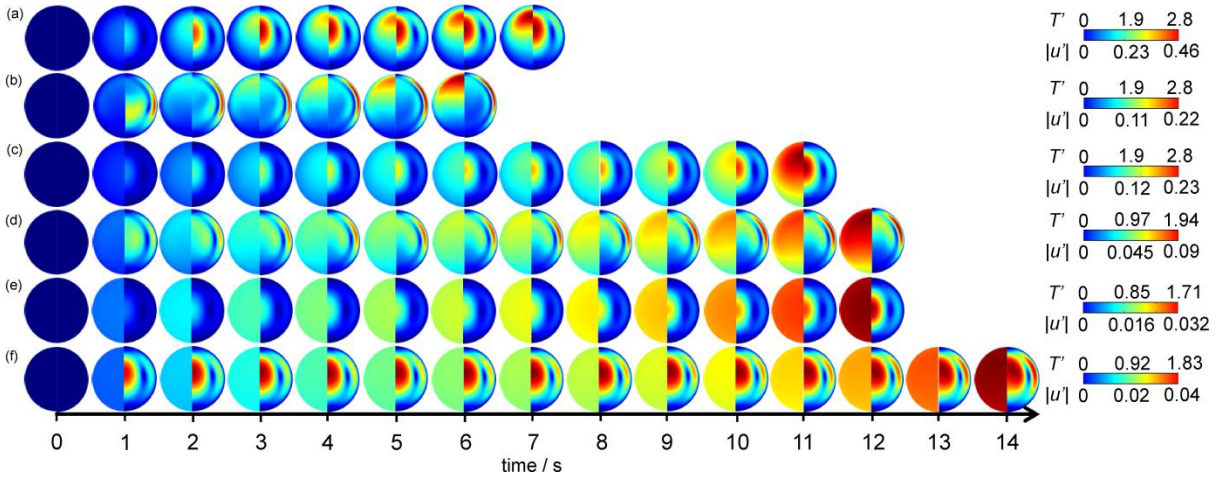


Figure 2. The temporal development of the spatial dimensionless temperature (left semi-circle) and speed (right semi-circle) profiles in the reactor for explosive cases very close to the explosive limit when (a) *Bi* = 10, *Ra* = $10^3$, (b) *Bi* = 10, *Ra* = $10^5$, (c) *Bi* = 1, *Ra* = $10^3$, (d) *Bi* = 1, *Ra* = $10^5$, (e) *Bi* = 0.1, *Ra* = $10^3$ and (f) (*Bi* = 0.1, *Ra* = $10^5$. The times are given in dimensional units for ease of comparison and indicative colour scales are given on the right.

In Fig. 2(a) it is clear that the system heats up due to the reaction and a hot zone begins to form above the centre of the reactor at *t* = 2 s. In this case there is weak natural convection and this is what displaces the hot zone towards the top of the reactor. As the gas heats up, its density decreases and the higher temperature, lower density gas near the centre of the reactor experiences buoyancy forces which cause it to move vertically upwards. This high speed zone at the centre of the reactor is evident for *t* > 2 s. As the hot gas moves vertically upwards it contacts the cold wall and hence begins to descend, cooling further as it goes. This moderately high speed gas descending near the wall is also evident in Fig. 2(a). In the bottom half of the reactor, the density gradients are intrinsically stable and so the buoyancy forces are small, as are the velocities. There is also a large region of relatively cold gas, in fact close to the initial temperature, near the bottom of the reactor. As the reaction proceeds, the hot spot in the reactor shifts further up the vertical axis and eventually the explosion initiates in this hot region. Interestingly, there is evidence for all times shown in Fig. 2(a) of a thin thermal boundary layer at the top of the vessel which remains close to the initial temperature. This is despite the fact that the wall temperature is no longer held constant due to the existence of external heat transfer.

Shown in Fig. 2(b) is an explosive case where *Bi* = 10 and *Ra* = $10^5$. It can be seen that the temperature in the vessel increases relatively uniformly over the first second of reaction, and thereafter a hot zone forms close to the top of the vessel. This hot zone can be seen to develop for *t* > 2 s. As the convection is much more intense than that shown in Fig. 2(a), the hot zone is much closer to the top of the reactor. Additionally, the familiar horizontal stratification of the temperature, which is characteristic of cases when natural convection is significant, is evident. Due to the more intense convection and the proximity of the hot zone to the top of the reactor, the thermal boundary layer at a temperature close to the initial temperature, as seen in Fig. 2(a) for all times, persists only for the first 3 s of reaction. After that, it is evident that the intense natural convection, coupled to the removal of heat externally leads to the wall of the vessel heating up. The speed profiles show that as the vessel warms uniformly at the beginning of the reaction, there is significant upflow around the centreline of the reactor, and the warm gas descending along the cold walls moves very rapidly. Indeed, Fig. 2(b) shows that the flow in the thin layer close to the wall is very fast compared to the central up flow for *t* > 2 s. Interestingly, these temperature and velocity fields are structurally very similar to those presented previously (Liu *et al.*, 2008) for explosive cases with a constant wall temperature. This is perhaps unsurprising given that when *Bi* = 10, the internal heat transfer will still largely control the overall heat transfer. As mentioned above, the principal difference between Figs. 2(a) and (b) and their constant wall temperature counterparts is the erosion of the thermal boundary layer near the top of the vessel, due to the variation in the wall temperature that accompanies the external heat loss.

If the heat transfer coefficient describing heat loss from the external wall is decreased, then *Bi* will also decrease. Shown in Fig. 2(c) is the case where *Bi* = 1 and *Ra* = $10^3$ *i.e.* the internal and external heat transfer resistances are of similar order and natural convection is just becoming significant. The temporal development of the temperature shows a similar pattern to that in Fig. 2(a), with the temperature increasing approximately uniformly over the entire cross section of the reactor over the first 2 seconds of reaction before a hot zone develops above the centre of the reactor due to the effects of the convection. The

location of this hot zone is similar to that in Fig. 2(a), which is to be expected given the similar intensities of natural convection. The shape of the temperature contours is also qualitatively similar in the two cases. Where Fig. 2(a) and (c) differ though is in the magnitude of the temperature gradients. Whilst the case with $Bi$ = 10 in Fig. 2(a) shows a cold zone, with a temperature close to its initial value, toward the bottom of the reactor and around the wall, when $Bi$ is decreased in Fig. 2(c) then these regions show significant warming. There is therefore still spatial variation in the temperature in this case, but the gradients are considerably smaller. If the development of the velocity field is examined there is again some similarity to what is seen in Fig. 2(a) *i.e.* there is an area of higher speed that develops in the centre of the reactor after approximately 1 s of reaction and a region of higher speed flow near the wall. It is interesting to note that this downflow close to the wall takes longer to develop in this case than it does for the higher $Bi$ case. This is most likely due to the fact that the wall temperature is much larger in Fig. 2(c) than in Fig. 2(a) and therefore the descending gas is cooled less and so is less dense and hence there is less of a buoyancy driving force for downflow.

Figure 2(d) shows the development of temperature and speed for $Bi$ =1 and $Ra = 10^5$. It can be seen form Fig. 2(d) that the temperature increases virtually uniformly over the entire cross section of the reactor for the first 3 s, with only a small cold zone existing toward the bottom of the reactor. Subsequently, the hot zone begins to develop close to the top of the reactor. Its location is very similar to that seen in Fig. 2(b) for $Bi$ = 10, but as was the case for the low $Ra$ system at $Bi$ = 1, the variation in temperature throughout the reactor is much less than in the higher $Bi$ cases. Thus, the hot zone in Fig. 2(d) (*e.g.* at $t$ = 12 s) is much larger than that seen in Fig. 2(b) (*e.g.* at $t$ = 6 s). The development of the speed in Fig. 2(d) in comparison to that in Fig. 2(b) is also interesting. In both cases after ~ 1 s a region of relatively strong upflow develops about the centreline. Subsequently, a region of faster downflow along the wall in the upper half of the vessel emerges. It is interesting to note that the extent of this region is much less in the case of $Bi$ = 1 in Fig. 2(d) than when $Bi$ = 10 in Fig. 2(b). As discussed above, this is most likely due to the higher wall temperature that exists in the lower $Bi$ case. As the flow field develops in Fig. 2(d) it is clear that flow near the vertical axis in the top half of the vessel is more significant than was the case for $Bi$ = 10.

Figure 2(e) shows $Bi$ = 0.1 and $Ra = 10^3$. When $Bi \ll 1$, the temperature within the system is expected to be approximately spatially uniform. It is evident from Fig. 2(e) that this is indeed the case. Virtually no gradients in the temperature are visible. The development of the speed is similar to the previous cases with $Ra = 10^3$ in that there is a higher speed region around the centreline. It can be seen that this region is not however shifted towards the top of the reactor as is the case in Fig. 2(a) and (c). This is obviously because there is not a hot zone formed above the centre of the reactor, rather the temperature is uniform over the whole cross section. In Fig. 2(f) is the case with $Bi$ = 0.1 and $Ra = 10^5$. As in the low $Ra$ case, the temperature can be seen to develop similarly across the entire cross section. The velocity field is established in the first second of reaction and then changes very little. The intense mixing of course contributes to the spatial uniformity in temperature.

## The Effect of *Bi* on the Maximum Temperature in a Stable System

It was shown above that the primary difference between the temporal developments of the maximum temperature in stable systems as $Bi$ varied was the final temperatures reached, with lower temperatures occurring for lower values of $Bi$. There also seemed to be little difference between the cases at fixed $Bi$ as $Ra$ varied. To elucidate further these effects, simulations were performed to capture the maximum temperature that occurs in the steady state for a stable solution on the explosion boundary. This was done for a range of $Bi$ and at three values of $Ra$, *i.e.* $10^3$, $10^4$ and $10^5$. The results are plotted in Fig. 3.

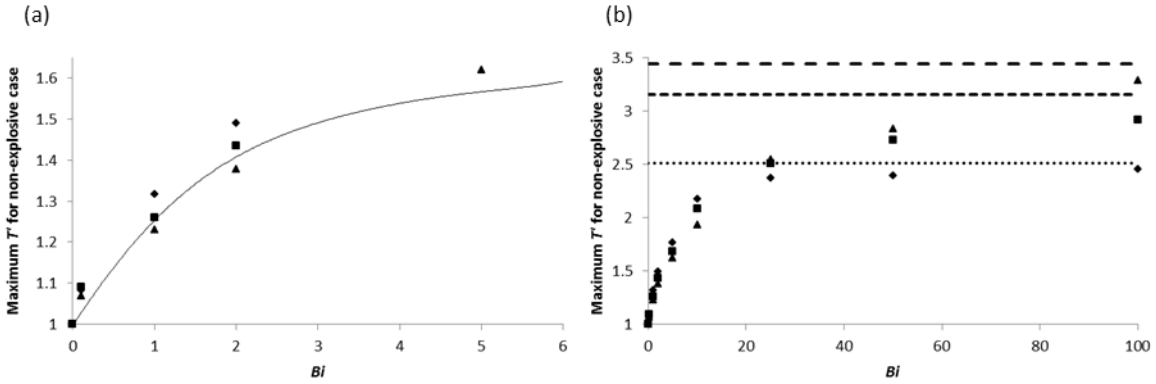


Figure 3. The maximum temperature in the reactor at steady state found numerically for a stable system on the explosion boundary as a function of $Bi$ and $Ra$. Part (a) shows $Bi$ < 6, whilst part (b) shows $Bi$ < 100. The diamonds are for cases with $Ra = 10^3$, the squares represent $Ra = 10^4$ and the triangles are $Ra = 10^5$. The solid line in (a) represents the analytical solution (Thomas, 1958) for the case without natural convection. Also plotted are horizontal lines which show the maximum temperatures for non-explosive cases with a constant wall temperature (*i.e.* $Bi = \infty$). The dotted line is for $Ra = 10^3$, the dashed line for $Ra = 10^4$ and the open dashed line for $Ra = 10^5$.

When $Bi$ = 0, the system is perfectly mixed and as predicted by Semenov, the maximum dimensionless temperature of a stable system is 1. When $Bi$ is increased, it is clear that there is an increase in the maximum temperature that can be achieved before explosion occurs. Indeed, for $Bi$ > 5, for the range of $Ra$ considered, it can be seen that the maximum temperature rises above the value of 1.6 that was predicted by Frank-Kamenetskii for a purely diffusive system. Interestingly, for each $Ra$

when $Bi$ < ~10 there is very little difference in the maximum temperatures achievable in a non-explosive case, and indeed it is clear from Fig. 3(a) that for $Bi$ < ~ 5, the maximum temperature is very close to that predicted analytically for a system without natural convection. It is interesting to note, however, is that the maximum temperature for each $Bi$ in this range is actually seen for the lowest value of $Ra$. This result is somewhat counterintuitive. Of course, it should be borne in mind that these maximum temperatures were derived numerically and the maximum temperature is sensitive to the proximity to the explosion boundary, nevertheless the trend is evident for all $Bi$ < 10. This trend is reversed as $Bi$ increases above 20, where the increased intensity of convection indicated by a larger $Ra$ results in a higher temperature being achieved in a stable reaction. When $Bi$ increases above 25, the maximum temperatures achieved diverge and the effect of the more intense convection is obvious. The maximum temperatures then clearly approach the values achieved in a constant wall temperature case (*i.e.* $Bi = \infty$) asymptotically. Thus, for $Ra = 10^3$, the maximum temperature is approximately 2.5, for $Ra = 10^4$ it is 3.15 and for $Ra = 10^5$ it is 3.45. Unsurprisingly, all three values are comfortably above the value of 1.6 suggested for diffusive systems, with a higher temperature being possible in a system with strong convection, due to the improved heat removal. Interestingly, all three values are below the $T^{\prime} = 5$ threshold suggested (Liu *et al.*, 2010) as a criterion for explosion in systems with considerable consumption of reactant. The most important consequence of the variation of the maximum temperature in a stable system with $Bi$ is that a simple criterion for explosion, based on a constant value of dimensionless temperature, may be inappropriate for cases with external heat transfer. This is a topic which clearly merits further study, when systems with significant consumption of reactant are investigated.

## Identification of Explosive Conditions as *Bi* varies

As has been shown above, the variation of external heat transfer, characterised by $Bi$, can have a significant effect on the behaviour of an exothermic reaction under the influence of natural convection. Of course, one of the most important questions that must be addressed is what effect does this external heat transfer resistance have on the tendency of a system to explode? To investigate this, many simulations were performed to find the boundaries of the explosive region for different values of $Bi$. These limits are summarised in Fig. 4, which shows a regime diagram plotted on logarithmic scales.

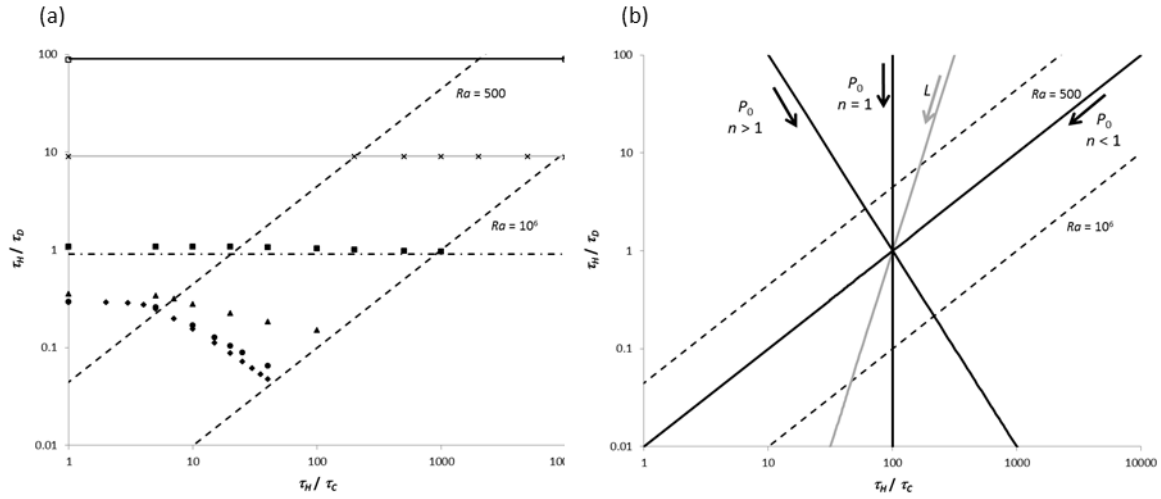


Figure 4. (a) The regime diagram for explosion showing the numerically derived explosion limits (for $Ra < 10^6$) for a range of $Bi$. Also shown are two dashed lines which show constant values of $Ra$. The diamonds show the limit for $Bi = \infty$, the circles show $Bi$ = 100, the triangles $Bi$ = 10, the squares $Bi$ = 1, the crosses $Bi$ = 0.1 and the open squares $Bi$ = 0.01. The horizontal lines show Semenov's prediction, *via* equation (20), for the explosive limit in a well-mixed system with varying $Bi$. The dot-dash line shows equation (20) for $Bi$ = 1, the grey line $Bi$ = 0.1 and the black line $Bi$ = 0.01. (b) The effect on the working point on the regime diagram of increasing the size of the reactor ($L$) as well as the initial pressure ($P_0$) for different orders of reaction $n$.

The boundary for $Bi = \infty$ agrees well with previous studies. The region below the boundary is where explosions occur, and that above it represents stable reactions. Two regions of behaviour are shown very clearly in Fig. 4(a). For $Ra$ < 500, diffusion dominates and the explosion limit is approximately constant. For $Ra$ > ~1000, then natural convection is important and there is clearly a power law variation in the explosion limit of the form

$$\left(\frac{\tau_H}{\tau_D}\right)_{explosion} \sim \left(\frac{\tau_H}{\tau_C}\right)^{\alpha} \tag{12}$$

where Liu *et al.* (2008, 2010). found this exponent to be -0.74 for $500 < Ra < 10^6$. The value found in this work is -0.82, which agrees reasonably well given the precision with which the boundary was found previously. Simulations for $Ra > 10^6$ (*i.e.* turbulent flows) have not been considered here, although the value of the exponent $\alpha$ has been predicted analytically (Liu *et al*., 2008) to be -2.

When a small amount of external heat transfer is allowed for (*i.e.* when $Bi$ = 100), it can be seen that for $Ra$ < 500, the explosion limit is virtually identical to that for the constant wall temperature case. As $Ra$ increases above 500 and natural

convection becomes more significant, it can be seen that explosions occur at a slightly higher value of $\tau_H/\tau_D$ than when *Bi* = ∞. This is of course due to the fact that the external resistance to heat transfer lessens somewhat the stabilising effect of the increased fluid flow and hence heat transfer from the contents of the vessel to the wall. It is also evident that the power law behaviour described in equation (12) still exists, though the value of the exponent is reduced.

For *Bi* = 10 it is shown in Fig. 4(a) that the critical value of $\tau_H/\tau_D$ in the diffusive region is increased slightly and that the stabilising effect of convection has been substantially lessened. For *Bi* = 1, there is still a very slight stabilising effect of convection evident for 500 < *Ra* < $10^6$, however for *Bi* < 1, the explosive limit has an approximately constant value of $\tau_H/\tau_D$. It is shown very clearly in Fig. 4(a) that external heat transfer has two main effects *viz.* it increases the critical value of $\tau_H/\tau_D$ indicating that the system is more prone to explode and it also lessens the stabilising effect of natural convection. The effect of some key process parameters on the location of the working point on the regime diagram is shown in Fig. 4(b). The initial pressure, which primarily affects the concentration of the reactive species influences both $\tau_H/\tau_D \propto P_0^{-n}$ and $\tau_H/\tau_C \propto P_0^{n-1}$. Thus an increase in the initial pressure will move the working point on the regime towards the origin and hence make the system more prone to explosion. The nature of this move depends on the order of the reaction, and three types of behaviour are shown in Fig. 4(b). Similarly, the size of the reactor will also impact on the behaviour of the system. In this case $\tau_H/\tau_D \propto L^{-2}$ and $\tau_H/\tau_C \propto L^{-1/2}$. Thus at fixed *Bi*, despite the increase in *Ra* which accompanies an increase in vessel radius, the decrease in surface area per unit volume moves the system towards the explosive region. A vessel on an industrial scale is therefore much more likely to produce turbulent natural convection, but also more likely to undergo thermal explosion. It should also be noted that *Bi* also depends on *L*, although the exact dependence of course is influenced by the nature of the heat transfer to the surroundings. If there is forced convection, then standard correlations state that the Nusselt number (and heat transfer coefficient) has the form $Nu = 2 + a\,Re^{1/2}\,Pr^{1/3}$ and so $Bi \propto L^{1/2}$. Unsurprisingly an increase in *L* leads to greater heat removal from the surface and therefore potentially moves the system in a safer direction. If the heat transfer is by natural convection, then the heat transfer coefficient has the form $Nu = 2 + a\,Ra^{1/4}/f(Pr)$ and hence $Bi \propto L^{3/4}$. In both cases, it is implied that the larger the vessel, the closer the system will be to the constant wall temperature case. The final parameter of note is the initial temperature. The primary effect of initial temperature is on the rate of the reaction, and thus an increase in temperature will reduce the timescale for heating and move the working point towards the origin of the regime diagram. This once again makes an explosion more likely.

The extent to which the stabilising effect of convection is suppressed can be characterised by the exponent in equation (12). The variation of this exponent is shown, as derived from a best-fit of the numerical results, in Fig. 5.

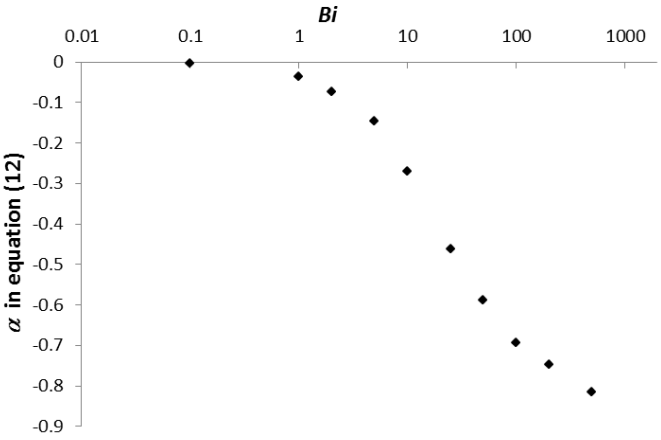


Figure 5. The exponent in equation (12), which characterises the stabilising effect of natural convection on the system, as a function of *Bi*.

Clearly, when *Bi* is very small, the explosive limit is approximately constant so $\alpha$ is close to zero. The bulk of the variation in $\alpha$ is seen over the range 1 < *Bi* < 100, which is similar to the range reported for main effect of *Bi* on explosion in diffusive systems with consumption of reactant (Boddington *et al.*, 1984). For *Bi* > 100, the value of the exponent in equation (12) approaches the *Bi* = ∞ value asymptotically.

## The Frank-Kamenetskii and Semenov Limits

The numerically derived explosion limits presented in Fig. 4 can be compared to analytical solutions in the Frank-Kamenetskii and Semenov limits. Frank-Kamenteskii (1969) derived an approximate expression for the transition to explosion in a purely diffusive system which can be written as

$$\left(\frac{\tau_H}{\tau_D}\right)_{explosionFK} = \left(\frac{\tau_H}{\tau_D}\right)_{Bi=\infty}\left(1+\frac{e}{Bi}\right). \qquad (13)$$

Plotted in Fig. 6 are the numerically derived explosive limits for a purely diffusive system and a line representing equation (13). There is clearly an excellent agreement between Frank-Kamenetskii's prediction and the numerical results. As observed above, the value of $\tau_H/\tau_D$ at the explosive limit is approximately constant for *Bi* > 10 and as predicted by equation (13) $\tau_H/\tau_D$ is proportional to $Bi^{-1}$ as *Bi* tends to zero and hence 1+ *e* / *Bi* tends to *e* / *Bi*.

Also plotted in Fig. 6 are the limits at different intensities of natural convection, specifically when $\tau_H/\tau_C = 10, 40$. It is clear that for *Bi* < 1, the explosive limit is largely independent of the degree of mixing due to natural convection. This is unsurprising as the heat transfer is dominated by the external processes, and the temperature in the vessel is approximately spatially uniform. For *Bi* > 1, the stabilising effect of convection, *i.e.* the reduction in the size of the explosive regime is evident.

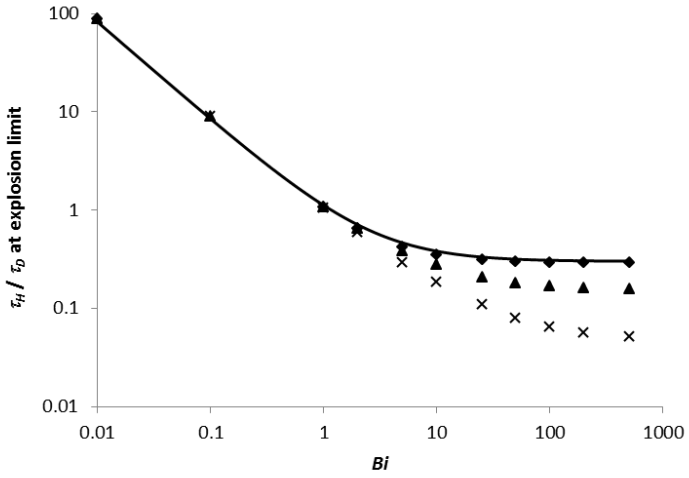


Figure 6. A comparison of the numerically derived explosion limit for a purely diffusive system for different values of *Bi* with Frank-Kamenetskii's approximate expression in equation (13). The diamonds are the numerically derived limits when $\tau_H/\tau_C = 0$ and the solid line represents equation (13). The triangles represent the transition when $\tau_H/\tau_C = 10$ and the crosses the transition when $\tau_H/\tau_C = 40$.

At small values of *Bi*, where external heat transfer is the dominant mechanism, the Semenov limit of a well-mixed system is approached. Semenov's prediction can be re-written in terms of the characteristic timescales used here as

$$\left(\frac{\tau_H}{\tau_D}\right)_{explosion,Semenov} = \frac{e}{3Bi}. \tag{14}$$

It is interesting to compare this with the form of equation (13) as *Bi* tends to zero. In this limit, equation (13) is approximated by

$$\left(\frac{\tau_H}{\tau_D}\right)_{explosionFK} \approx \left(\frac{\tau_H}{\tau_D}\right)_{Bi=\infty} \frac{e}{Bi} = \frac{1}{3.32}\frac{e}{Bi}. \tag{15}$$

which agrees well with equation (14). Equation (14) is plotted for *Bi* = 0.01, 0.1 and 1 in Fig. 4(a). For *Bi* = 1, equation (14) slightly under predicts the explosive limit and, of course, does not capture the marginal stabilising effect of convection. This discrepancy is unsurprising given that there is still some spatial variation in the temperature field. For *Bi* << 1, the agreement between equation (14) and the numerically derived boundaries can be seen to be excellent in Fig. 4(a), with the numerically derived results agreeing with Semenov's prediction to within 2%. This excellent agreement between the analytical predictions in both limits not only provides further validation of the numerical methods used, but also shows that the inclusion of external heat transfer in systems with natural convection truly bridges these two classical limits.

## Conclusions

The behaviour of an exothermic chemical reaction occurring in a spherical vessel under the influence of natural convection and an external heat transfer resistance, but without consumption of reactant, has been studied numerically. It has been shown that the external heat transfer, as characterised by a Biot number, has very little qualitative impact on the temporal development of the maximum temperature in the reactor during explosive and non-explosive reactions. The main quantitative effect is that the reactions take place at a lower temperature when *Bi* is reduced. Indeed, it has been shown that the maximum dimensionless temperature achieved in a non-explosive reaction on the explosion boundary increases from 1 in the well mixed limit to its constant wall temperature value asymptotically. For *Bi* < ~ 10, the maximum temperature varies little with Rayleigh number, but interestingly is lower for higher values of *Ra*. This is in contrast to what is observed at

higher *Bi* where more intense natural convection means that higher temperatures can be sustained in non-explosive cases. This effect may be due to the reduction in driving force for heat transfer from the hot zone of the reactor to the wall. This is primarily due to the fact that the wall temperature increases much more significantly as *Bi* is reduced. Importantly, this variation in maximum temperature achieved in stable systems means that explosion criteria based on the maximum temperature achieved in the reactor may be inappropriate for systems with significant external heat transfer.

A region of parameter space where explosions occur has been defined for a series of values of *Bi*. It has clearly been shown that the inclusion of external heat transfer means that the region of parameter space where explosions occur is larger and that the stabilising effect of natural convection on the reaction is greatly diminished as *Bi* is reduced, particularly over the range 100 – 1. Finally, the numerical results have been shown to agree very well with the analytical solutions of Frank-Kamenetskii and Semenov in the purely diffusive and well-mixed limits.

## Acknowledgements

The financial support of the Engineering and Physical Sciences Research Council *via* Small Equipment Grant EP/K031317/1 is gratefully acknowledged. This work is adapted from Campbell (2015) under licence (CC BY 3.0) from the PCCP Owner Societies.

Data Availability: The author confirms that all data underlying the findings are fully available without restriction. The data is held at the University of Surrey and requests for access can be sent to researchdata@surrey.ac.uk

## References

T. Boddington, C. Feng and P. Gray, *Proc. R. Soc. A*, 1984, **391**, 269 – 294.

A. N. Campbell, *Phys. Chem. Chem. Phys.*, 2015, **17**, 16894-16906.

COMSOL, COMSOL Multiphysics Reference Guide Version 4.3a, 2012.

D. A. Frank-Kamenetskii, *Diffusion and Heat Transfer in Chemical Kinetics 2nd Edition (ed. J. P. Appleton)*, 1969, Plenum.

D. R. Jones, *Int. J. Heat Mass Tran.*, 1973, **16**, 157 – 167.

T.-Y. Liu, A. N. Campbell, S. S. S. Cardoso and A. N. Hayhurst, *Phys. Chem. Chem. Phys.*, 2008, **10**, 5521 – 5530.

T.-Y. Liu, A. N. Campbell, A. N. Hayhurst and S. S. S. Cardoso, *Combust. Flame*, 2010, **157**, 230 – 239.

A. G. Merzhanov and E. A. Shtessel, *Combust. Explos. Shock Waves*, 1971, **7**, 58 – 65.

A. G. Merzhanov and E. A. Shtessel, *Astronaut. ACTA*, 1973, **18**, 191–199.

N. N. Semenov, *Z. Phys.*, 1928, **48**, 571-582.

P. H. Thomas, *Trans. Faraday Soc.*, **54**, 60 – 65.